EurJIC
European Journal of Inorganic Chemistry

Research Article
doi.org/10.1002/ejic.202300268

Chemistry Europe
European Chemical Societies Publishing

www.eurjic.org

Special Collection

Cooperative Dinitrogen Activation: Identifying the Push-Pull Effects of Transition Metals and Lewis Acids in Molecular Orbital Diagrams

Frederico F. Martins[b] and Vera Krewald*[a]

The sustainable fixation of atmospheric N_2 and its conversion into industrially relevant molecules is one of the major current challenges in chemistry. Besides nitrogen activation with transition metal complexes, a "push-pull" approach that fine-tunes electron density along the N–N bond has shown success recently. The "pushing" is performed by an electron rich entity such as a transition metal complex, and the "pulling" is achieved with an electron acceptor such as a Lewis acid. In this contribution, we explore the electronic structure implications of this approach using the complex *trans*-[Re^{I}Cl(N_2)(PMe_2Ph)$_4$] as a starting point. We show that borane Lewis acids exert a pull-effect of increasing strength with increased Lewis acidity via a π-pathway. Furthermore, the ligand *trans* to dinitrogen can weaken the dinitrogen bond via a σ-pathway. Binding a strong Lewis acid is found to have electronic structure effects potentially relevant for electrochemistry: dinitrogen-dominated molecular orbitals are shifted into advantageous energetic positions for redox activation of the dinitrogen bond. We show how these electronic structure design principles are rooted in cooperative effects of a transition metal complex and a Lewis acid, and that they can be exploited to tailor a complex towards the desired thermal, electrochemical or photochemical reactivity.

Introduction

The conversion of dinitrogen into a chemically useful form, ammonia, is responsible for nearly two percent of the total energy consumption of the world.[1] This shows the importance of reductive dinitrogen activation for modern human life. However, since the underlying Haber–Bosch process[2] requires large amounts of fossil energy and is associated with significant carbon dioxide emissions, this is not a sustainable route. The current industrial standard thus raises serious environmental concerns[3] despite the feedstock N_2 being virtually inexhaustible. As society ought to move towards reducing its carbon footprint, it is urgent to find more effective methods of utilizing atmospheric nitrogen and converting it into useful chemicals in a sustainable manner.[4] This need for change led IUPAC to choose "sustainable ammonia" as a top ten emerging technology in chemistry 2021.[5]

N_2 is challenging to activate due to its lack of a dipole moment, strong σ and π bonds with a dissociation enthalpy of ca. 225 kcal mol^{-1}, and high ionization potential of ca. 16 eV.[6] Despite these challenges, some bacteria are successful in catalyzing dinitrogen reduction at ambient conditions through nitrogenase enzymes, which contain FeMo- or FeV-cofactors as the active sites.[7] This fact motivated a large body of literature towards N_2 activation based on the study of iron and molybdenum transition metal complexes and clusters.[8]

Several recent reviews have highlighted the challenges and the progress in dinitrogen activation chemistry.[9] Besides bio-inspired studies, there have been many contributions on dinitrogen binding, activation and splitting using a broad range of transition metal complexes.[10] N_2 cleavage can be achieved via thermal,[8a,11] photochemical[12] or electrochemical[13] pathways. The thermal pathway is probably the most well-explored route with many different choices of transition metals, ligand design strategies, and reaction environments.[9b,c,11a,14] The photochemical and electrochemical pathways involve either the population of previously vacant N–N antibonding orbitals, or the depopulation of N–N bonding orbitals.

Focusing on the thermal pathway, one view of the reduction process is that electrons are "pushed" from the metal to the dinitrogen ligand, the extent of which depends on the metal acidity. This idea can be further expanded if an electron donor is bound to the metal,[15] thus increasing the "pushing" strength. The use of cooperative strategies in the design of transition metal compounds has proven extremely important for systems used in bond activation and catalysis and N_2 activation is no exception.[13a,16] Cooperativity can be achieved

[a] *Prof. Dr. V. Krewald*
Department of Chemistry, Theoretical Chemistry
TU Darmstadt
Peter-Grünberg-Str. 4, 64287 Darmstadt (Germany)
E-mail: vera.krewald@tu-darmstadt.de

[b] *F. F. Martins*
IQCC & Department Química
Universitat de Girona
Campus Montilivi (Ciències), 17003 Girona (Spain)

Supporting information for this article is available on the WWW under https://doi.org/10.1002/ejic.202300268

Part of the Special Collection on "Inorganic Reaction Mechanisms".

Research Article
doi.org/10.1002/ejic.202300268

in bimetallic complexes with two asymmetric metal coordination spheres,[17] with the idea that the resulting orbital interactions and electronic structure will allow for new modes of activation. A few heterobimetallic complexes (metal oxides), with the heavy metal combinations Re/Ti[18] or Re/Mo[19] have been reported to weaken the N_2 bond. However, to the best of our knowledge, the only heterobimetallic complexes with an N_2 bridge and first-row transition metal complex that have been synthesized are the much more recent chromium and iron Re-N_2-metalloporphyrins reported by Zhang and coworkers.[20]

A different strategy exploiting cooperativity relies on Lewis Acids (LAs). A Lewis acid is defined by IUPAC[21] as an electron pair acceptor, and this ability can in principle contribute to the weakening of adjacent chemical bonds. In fact, Lewis acids have been reported to have a "pulling" capability,[22] making them viable candidates for building blocks in cooperative molecular entities: a transition metal complex is used as an electron donor and a Lewis acid as an electron acceptor.[23] This so-called "Push/Pull" strategy has proven quite successful in the weakening of the N_2 bond, in particular with borane Lewis acids,[24] as the sp^2 orbital of boron is vacant and thus may take electron density from the dinitrogen bridge while the filled p orbital is implicated in π-backdonation.[25] This mechanism had originally been proposed for nitrogenase,[7] where the positive charge in sulfur-bound hydrogen species enhanced the pushing of electrons by the cofactor into the dinitrogen molecule. Furthermore, bis-borylene activation of dinitrogen without a transition metal complex is known,[26] and similarities may be drawn with the frustrated Lewis pair strategy for metal-free dinitrogen activation.[27]

In this work, we revisit the Re^{I} complex synthesized by Chatt (Figure 1).[28] It can form dinuclear, N_2-bridged complexes; adducts were obtained with group 4, 5 and 6 halides[18,29] and metalloporphyrins.[20] Furthermore, the co-activation by Lewis acids has been studied before in the Fe^0 and Re^{I} cases.[23b,c] Herein, we set out to rationalize how the addition of Lewis acids as a second molecular entity to the distal end of the N_2 molecule affects the dinitrogen bond strength for mononuclear transition metal complexes. Ideally, a metal complex with a Lewis acid co-activator would be less expensive, but at least equally effective and perhaps even more adaptable. Since Mo^0 and W^0 complexes with phosphine equatorial ligands have been shown to spontaneously bind two dinitrogen units and work as templates for further functionalization,[30] or direct conversion of dinitrogen into ammonia,[31] we also study the isoelectronic molybdenum and tungsten analogues of the Chatt complex.

We quantify the degree of dinitrogen activation via different pathways and rationalize the LA effect in terms of the bonding situation. Additionally, we discuss to which extent substituting the chloride ligand can further weaken the dinitrogen bond. The complexes suggested herein and the orbital-based mechanisms for dinitrogen activation may prove helpful for the design of cooperative molecular systems capable of chemically transforming dinitrogen or other small molecules.

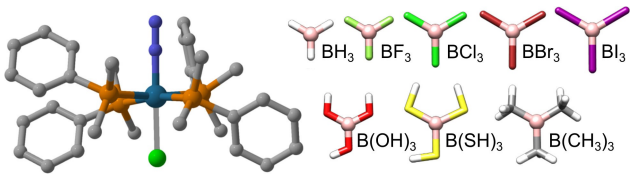

Figure 1. Molecular structures of the parent complex, *trans*-[Re^{I}Cl-(N_2)(PMe_2Ph)$_4$], (left) and some of the Lewis acids tested in this work (right). The geometries of the bulkier acids $B(C_2F_5)_3$, $B(OTf)_3$, BPh_3, $B(C_6F_5)_3$, $B(N(C_6F_5)_2)_3$ are shown in the SI, Scheme S1. The color code of the elements is rhenium, teal; nitrogen, blue; phosphorus, orange; carbon, grey; chloride, green; fluoride, light green; bromide, dark red; iodide, purple; oxygen, red; sulfur, yellow; hydrogen, white; carbon-bound hydrogen atoms are omitted for clarity.

Results and Discussion

Assessing the Extent of N_2 Activation

While the chemical concept of an "acceptor of electrons" is rather intuitive, the quantitative determination of Lewis acidity is not a trivial chemical problem[32] even though it is in principle rooted in thermodynamics.[33] In this work, the fluoride ion affinity (FIA) was used as a Lewis acidity descriptor. The computational approach chosen with some background information and a comparison with the hydride ion affinity (HIA), can be found in the Supporting Information. To understand how the LA affects the molecular orbitals (MOs) involving the dinitrogen unit, we analyzed the MO diagram of the bare Re-N_2 complex. The energy of the δ orbital, a relatively pure atomic orbital with rhenium $d_{x^2-y^2}$ character, is used as a reference point for frontier orbitals with significant rhenium or dinitrogen character.

Previously reported metal-dinitrogen MO diagrams for linear M–N–N–M and M–N–N complexes showed considerable splitting between σ-bonding and σ^*-antibonding interactions while the remaining π interactions were found closer to the frontier orbital region.[8a,11a,34] In the present case, the σ-type orbitals[35] are HOMO-15 and LUMO + 16 (Figure 2). The δ reference orbital

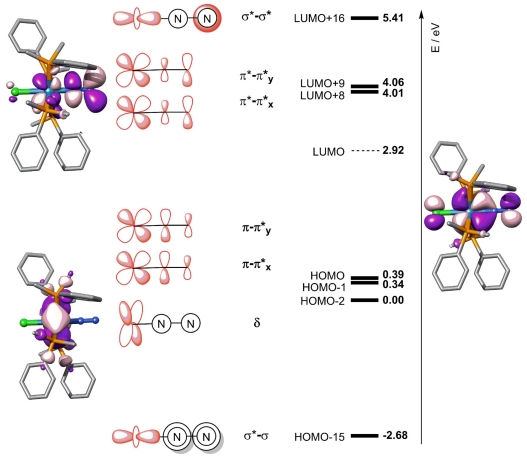

Figure 2. The MO diagram of the parent Re^{I} complex focusing on the orbitals with dominant metal and nitrogen character. Note that the orbital energies shown here are energies in eV relative to the δ reference orbital, HOMO-2.

Research Article
doi.org/10.1002/ejic.202300268

of the bare complex is found in the HOMO-2 position. The frontier occupied orbitals, HOMO and HOMO-1, have π-antibonding character for the N–N bond due to π-backbonding, which suggests that oxidation should increase the strength of this bond. Reduction of the complex would likely not weaken the N–N bond since the LUMO is found to comprise the aromatic π-systems of the phenyl rings in the phosphine ligands. The π*–π* orbitals are rather destabilized (3.62 eV above the HOMO).

The LAs selected are shown in Figure 1 and the SI. This particular set of boranes was chosen to generate a broad range of values within the Lewis acidity scale. Computational chemistry allows us to interrogate chemical space that has not been accessed experimentally to aid in the understanding of general chemical phenomena and this is the aim of the current work.

To study the effect of LA binding towards a strategic influence of the molecular orbitals and thereby the degree of dinitrogen activation, the thermodynamic stability of Lewis Acid adducts of the rhenium complex and the analogous tungsten and molybdenum complexes with the same d configuration is evaluated. The formation of the LA adducts is generally thermodynamically favorable with stabilization energies between −15 and −241 kJ mol^{-1} (see Supporting Information Table S3 for complete data sets), although no clear trend can be obtained likely due to a taut balance between electronic and steric effects. Exceptions to this are $B(OH)_3$ (ca. +32 kJ mol^{-1}) and $B(N(C_6F_5)_2)_3$ (ca. +220 kJ mol^{-1}) for all three metal centers, and for Re^I additionally $B(CH_3)_3$ and $B(SH)_3$. We hypothesize that $B(OH)_3$ is not a strong enough electron acceptor to establish a proper bond with end-on-bound dinitrogen. For $B(N(C_6F_5)_2)_3$, the electrostatic repulsion between the bulky LA and the metal complexes may surpass any stabilization resulting from bonding, rendering the putative N–B bond unstable. For the cases of $B(CH_3)_3$ and $B(SH)_3$ adducts with rhenium, we do not have a simple explanation.

The Lewis acids bind the end-on nitrogen ligand via the boron atom, forming a non-linear Re-N–N-LA subunit with the N–N···B angle varying from 132° (BF_3) to 172° ($B(CH_3)_3$). This geometrical arrangement is reminiscent of a dinuclear bent bridging motif[36] and may allow for an electrophilic attack of a substrate on the nascent lone-pair at the boron-bound nitrogen atom. The N–N bond distance in the bare Re-N–N complex is 1.154 Å, and it ranges from 1.158 Å [$B(CH_3)_3$] to 1.208 Å [$B(OTf)_3$] in the Re–N_2–LA adducts, suggesting some degree of bond weakening for all adducts. While the strength of a bond is often assessed by the bond length, it can be evaluated more quantitatively with other parameters such as bond orders or N–N stretching frequencies.[37] To compare the validity of these measures, N–N Mayer bond orders and $\upsilon_{N-N(stretch)}$ frequencies are plotted against the calculated FIA in Figure 3. Additionally, NBO analyses of three representative adducts are presented in the SI (Table S5).

Figure 3a shows that the N–N bond orders of the metal complex-LA adducts (dots) are lower than in the bare complexes (dashed lines), indicative of a higher degree of N_2 activation. However, the values are rather scattered across the

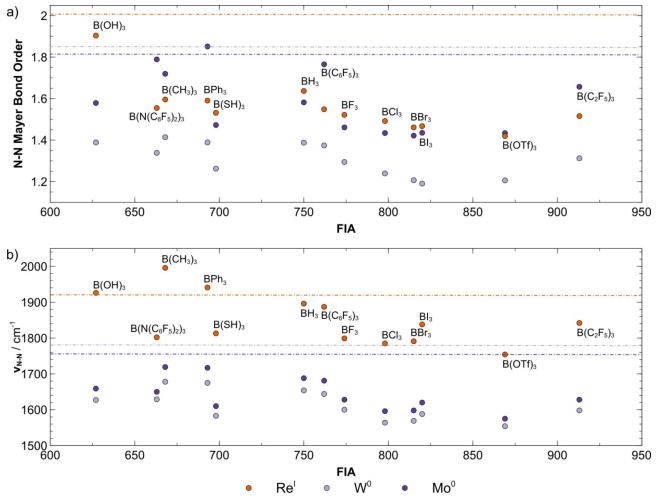

Figure 3. Computed a) N–N Mayer bond orders and b) N–N vibrational frequency *vs.* calculated FIA. The data points represent different metal ion-LA adducts: Re^I (orange), W^0 (purple) and Mo^0 (light purple). Dashed lines represent the values of the bare complexes. An analogous picture with HIAs instead of FIAs can be found in the Supporting Information, Figure S3.

FIA scale and do not show a clear trend for the three metal elements studied so that Mayer bond orders should be interpreted with some caution. The N_2 stretching frequencies shown in Figure 3b show a general decrease of υ_{N-N} with increasing FIA, although not in a reliably predictive manner, and a clear trend for the three types of central metal. Deviations from linearity along the FIA scale may be due to steric effects: the relationships between υ_{N-N} and FIA for LAs with comparable steric hindrance, such as the $B(OH)_3$/$B(SH)_3$ and BPh_3/$B(C_6F_5)_3$ pairs, appear to be reasonable. The case of $B(C_2F_5)_3$, however, does not follow this trend. Its structure is very similar to that of the $B(OTf)_3$ adduct, so considering that a higher FIA was obtained in both our computational model and that of Greb and coworkers, a decrease in υ_{N-N} is expected. We will return to this result further below as it may be related to the molecular orbitals resulting from adduct formation (Figure 4).

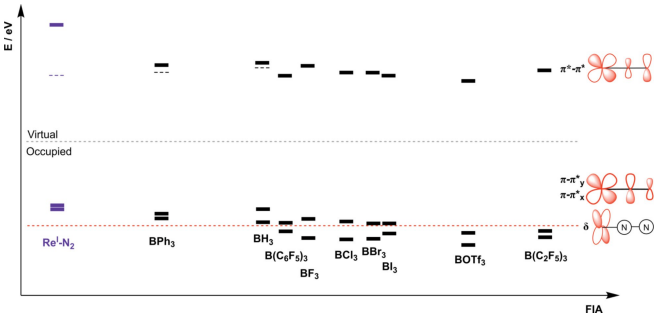

Figure 4. Molecular orbital energies of the occupied π–π* and virtual π*–π* orbitals relative to the respective δ orbital energies (orange dashed line) for all LA-N_2-rhenium(I) adducts. The bare complex is represented in purple and the Lewis acids with thermodynamically unfavorable binding in orange, except $B(OH)_3$ as no stable structure with a B–N bond was obtained. Orbitals that do not have considerable N character are not represented unless they correspond to the LUMO (dashed lines).

We note that the decrease in $\upsilon_{N-N(stretch)}$ with increasing FIA is independent of the metal ion – the "pushing" of electrons into the N_2 bridge is consistent for all adducts and depends only on the acidity of the metal. This is an important finding as orthogonal effects can be independently tuned and exploited for the rational design of new molecules. Binding to the electron withdrawing Lewis acids can weaken the N–N bond from an obvious triple bond[37] in the bare Re^I complex with a N–N stretching mode at 1919 cm^{-1}, to 1754 cm^{-1} in the Re^I–$B(OTf)_3$ adduct or even to values as low as 1575 cm^{-1} for the analogous Mo^0-$B(OTf)_3$ complex. These stretching frequencies are consistent with the N–N double bond range (ca. 1300–1800 cm^{-1}), and are much lower than those reported, for instance, for the Re^I–N_2-metalloporphyrin complexes of iron and chromium (1803 and 1887 cm^{-1}, respectively).[20] We note that the predicted modes are expected to differ from experimental values due to the harmonic approximation and intrinsic DFT errors. The qualitative trend and the degree of activation, however, is expected to translate to experimental observations. Our findings are in general agreement with those of Szymczak and coworkers for an Fe^0 model of the nitrogenase enzyme and the Re complex,[23b,c] although for a smaller range of Lewis acids. This result strongly supports the usefulness of LAs for electronic structure modulations and implies that a more detailed electronic structure analysis can shed light onto the activation mechanism in M-N_2-LA adducts.

Electronic structure modulation

Having shown that the formation of M–N_2–LA adducts affects the N–N bond strength, the findings will now be interpreted within an MO framework for the series of Re–N_2–LA adducts. $B(OH)_3$ is excluded from this analysis because no stable structure with a B–N bond was found.

Szymczak and coworkers[23b,c] rationalized the decrease in υ_{N-N} by comparing the admixture of $d_{xy}/d_{xz}/d_{yz}$-type atomic orbitals of the transition metal with π-MOs of the N_2-LA adduct and discussed the stabilization of the resulting MOs with respect to the MOs of the separate fragments. We did not find a significant variation of the rhenium atomic orbital coefficient in the π-frontier MOs (values ranging from 2.7% to 5.2%). We also found no meaningful correlation between the degree of admixture and the calculated FIAs or υ_{N-N} for the complexes studied here.

We therefore devised an alternative approach for rationalizing the LA effect in an MO framework. As a suitable reference point for comparing orbital energies across all M-N_2-LA adducts, we chose the Re $d_{x^2-y^2}$ orbital (δ-MO), since it can be readily identified, corresponds to an essentially pure Re atomic orbital and should thus not change its energy when adduct formation occurs. This approach is advantageous as it only requires a description of the full adduct and not of the separate fragments.

Figure 4 shows how the electron withdrawing capabilities of the LAs affect the frontier orbital energies in the adducts relative to the δ-MO. The relative energies of the π–π* orbitals generally decrease with increasing FIA, in a very similar trend to that observed in Figure 3 for the N–N stretching frequencies. Correlating the energy of the more stable π–π* orbital against υ_{N-N} shows a linear relationship with a coefficient of determination R^2 close to 0.80. The mean absolute error is quite small, −0.09 eV. The elimination of the four adducts that are not thermodynamically stable ($B(N(C_6F_5)_2)_3$, $B(SH)_3$, $B(OH)_3$, $B(CH_3)_3$) leads to an improvement of the coefficient of determination to 0.95 and a much better correlation ($E_{\pi-\pi^*} = 0.0027\upsilon_{N-N} - 5.0912$ eV). A very similar trend is observed if instead of the energy of the lower π–π*, the center of gravity of the two π–π* orbitals is considered (albeit with a smaller R^2 value of 0.80).

These results show that the weakening of the N–N bond by a LA, usually referred to as a "pulling" effect, can be interpreted within the MO scheme as a stabilization of the π–π* orbitals upon formation of the adduct. In contrast, the π*–π* orbitals are essentially unaffected by LA binding.

It is also noteworthy that, in contrast to what had been observed upon plotting υ_{N-N} vs FIA (Figure 3), the expected relative positions of $B(OTf)_3$ and $B(C_2F_5)_3$ are obtained in Figures 4 and 5. This may be interpreted as a more favorable overlap between the π orbitals of dinitrogen with those of $B(OTf)_3$ compared to those of $B(C_2F_5)_3$ that outweighs the apparently weaker electron withdrawing capability of $B(OTf)_3$.

Implications for electrochemistry

Although the π*–π* orbital energy is essentially the same in all adducts, see Figure 4, an important observation is that the stronger Lewis acids shift the π*–π* orbital into the LUMO position. This may allow its population via electrochemical reduction, which would decrease the strength of both the metal-nitrogen and the nitrogen-nitrogen π-bonds. Even though it was not rationalized within a molecular orbital framework, the facilitation of redox catalysis via binding to an electron acceptor has already been achieved in the context of

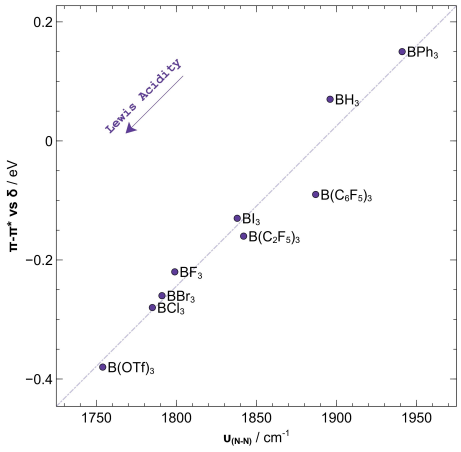

Figure 5. Relative energy of the lower π–π* orbital with respect to the metal δ orbital, for each Re^I-N_2-LA adduct, plotted against the respective N–N stretching frequency. Linear fit parameters: $y = 0.0027x - 5.0912$, $R^2 = 0.9491$.

Research Article
doi.org/10.1002/ejic.202300268

dinitrogen binding and functionalization.[38] That a change in redox potential occurs upon LA binding was also seen by Szymczak and coworkers.[23b] A dual effect of LA co-activation coupled to electrochemical reactivity could contribute to the desired result of forming bonds between nitrogen and a new organic unit or to releasing the product from the metal.

The nature and energy of the required electrochemical steps to further enhance N_2 activation was evaluated by calculating the redox potentials and anchoring them to an experimentally measured reversible redox peak in a Re^{I} analogue.[39] The processes studied here are shown in Scheme 1 with redox potentials *vs.* SHE for the parent complex. A constant of 0.244 V was added to the potentials in order to move from the SCE (experimental result) to SHE scale.

The metal ion was confirmed to undergo the oxidation processes, as the appropriate spin density changes are solely accumulated on the rhenium atom (see Supporting Information). The reduction, however, is shared between the phosphine aromatic systems and the rhenium ion (weak LAs) or between the nitrogen bridge and the rhenium ion (strong LAs), as expected from the nature of the corresponding LUMOs.

While the expected spin states for the Re^{0-II} species are clear, there are two plausible spin states for Re^{III}. Calculations show that the singlet state is energetically preferred over the triplet state for the bare complex (−10 kJ mol^{-1}) and LA adducts (BPh_3: −1 kJ mol^{-1}; $B(C_2F_5)_3$: −4 kJ mol^{-1}; others: −10 to −14 kJ mol^{-1}). Considering these small energy differences and expected spin-orbit coupling effects suggests that the redox potentials predicted here will likely differ from those that would be measured experimentally. However, even with this uncertainty in mind, the calculated redox potentials reported in Table 1 seem attainable and are in agreement with previous reports for similar Re-N_2 complexes.[39]

$$Re^{0} \xleftarrow{-2.39} Re^{I} \xleftarrow{0.42} Re^{II} \xleftarrow{1.47} Re^{III}$$

Scheme 1. Computed reduction potentials between the different rhenium species (bare complex) vs SHE (V).

Table 1. N–N stretching frequencies (cm^{-1}) and reduction potentials (V vs. SHE) for the different rhenium oxidation states and adducts. The data for Re^{III} species is based on singlet spin states.

	LA	Re^0	Re^I	Re^{II}	Re^{III}
υ(N–N) [cm^{-1}]	–	1897	1919	1993	2074
	BPh_3	1907	1941	1978	2038
	BH_3	1847	1896	2009	2112
	$B(C_2F_5)_3$	1514	1842	1911	1985
	BCl_3	1514	1785	1860	1975
	$B(OTf)_3$	1467	1753	1837	1884
Pot. vs SHE [V]	–	−2.39		0.42	1.47
	BPh_3	−2.31		0.74	1.78
	BH_3	−2.32		0.72	1.64
	$B(C_2F_5)_3$	−1.97		1.14	2.24
	BCl_3	−1.94		1.20	2.07
	$B(OTf)_3$	−1.73		1.38	2.27

The results completely corroborate the expectations from the molecular orbital analysis shown in Figure 4. For the LA adducts with a π*–π* orbital as the LUMO, ($B(C_2F_5)_3$, BCl_3 and $B(OTf)_3$), reduction to Re^0 decreases the N–N stretching frequency by ca. 300 cm^{-1}. This is not observed for the bare complex or the ones forming adducts with BPh_3/BH_3, because the π*–π* orbitals are not in the frontier region (LUMO + 8). The weakening of both the Re–N and N–N bonds upon reduction is also corroborated by the increased bond lengths of the reduced complexes relative to the neutral compounds. In the case of the Re–N_2–$B(OTf)_3$ adduct, the increase is similar for the Re–N (0.078 Å) and the N–N (0.050 Å) bonds.

Single and double oxidation events lead to an increase in υ_{N-N}, as the antibonding π–π* HOMO orbital is depopulated. Not only does the binding to LAs allow for a reduction process productive for nitrogen bond weakening, but it also shifts the redox level (ca. +0.8 V) towards better attainable potentials, making this reduction easier while maintaining the redox span. The latter shift had also been reported for the Fe^0 nitrogenase-like complex.[23c]

trans influence

As a final tuning opportunity in the complex, the ligand in the *trans* position to the nitrogen bridge[40] was modified to study a putative enhancement of the "pushing" effect of the metal, possibly leading to cooperative pushing and pulling. The "push" had previously been rationalized as the donation from filled metal *d* orbitals to N_2 π* orbitals upon formation of the M–N_2–LA adducts.[23c] We thus tested the substitution of the chloride ligand in the initial rhenium complex with the other halogens. We chose a halogen series as a chemically similar and spectrochemically well understood series. We expect σ donor and π acceptor ligands to considerably shift the MO arrangement. Szymczak and coworkers showed competitive binding of four borane LAs to the halogen,[23b] and hence we calculated the energy difference between the expected LA–N binding and LA–X binding for three LAs of different ends of our dataset (BPh_3, $B(C_2F_5)_3$, $B(OTf)_3$, see Supporting Information). We confirmed the two types of adduct to be isoenergetic, meaning that in similar application cases the preference of one form over the other may be subtly influenced by the ligand design and specific environmental effects in the experiment. The following results may thus be qualitatively correct, but not quantitatively accurate or quantitatively transferrable to other complexes.

An increasing halogen electronegativity decreases the N–N stretching frequency in the three test cases shown in Figure 6. This suggests that removing electron density from the metal ion improves N–N activation, contrary to what had previously been reported for complexes with *trans* boron-metal bonds and is expected for a "push"-like effect. The effect is small for Cl, Br and I (ca. 5–10 cm^{-1} per halide substitution step), but when chloride is substituted by fluoride, a decrease comparable to the pulling effect of the Lewis acids of up to 44 cm^{-1} is seen.

Research Article
doi.org/10.1002/ejic.202300268

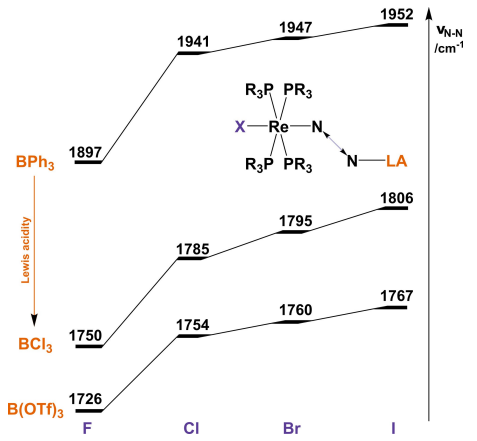

Figure 6. Effect of halogen substitution in the position *trans* to the dinitrogen bridge on different Lewis acid-bound Re^{I} complexes.

We note that binding of a LA and substitution of a *trans*-ligand are two independent processes, as the same effect is observed for three LAs at different points of the FIA spectrum, and can thus be exploited cooperatively.

This finding was rationalized with a molecular orbital diagram in which metal and halogen atoms are varied, see Figure 7. Taking the chloride complexes as a starting point (purple lines), it is shown how the π and σ orbitals along the halogen-metal-nitrogen axis are affected (i) by adduct formation with the strongest LA $B(OTf)_3$ (black lines), and (ii) additional substitution of the chloride ligand for the more electronegative fluoride (orange lines). For all three metals, the same π-stabilization is observed upon LA binding: the black energy levels of the LA adduct are lower in energy than the purple lines of the parent complexes.

Comparing the metal series from the more acidic Re^{I} to the less acidic Mo^{0}, the relative energies of the π frontier orbitals generally decrease. This is expected as the latter should be able to push more electron density into the N_2 antibonding orbitals and is in perfect agreement with the υ_{N-N} relationships established in Figure 3. We note that for the tungsten and molybdenum complexes, the π*–π* stabilization observed upon LA binding is similar to that discussed above for the rhenium complex. The π*–π* levels lower from LUMO + 9 to LUMO + 8, but the effect is not strong enough to create LUMOs of predominant N π* character and thus allow for productive reduction processes.

Importantly, upon substitution of the *trans*-ligand in the adducts, the π frontier orbitals are slightly destabilized due to π-donor effect of the halides.[23c] However, noting that the F–M–N_2–LA adducts have a smaller υ_{N-N} it is clear that the influence of the σ interaction must be more important. Inspection of the σ bonds along the X–M–N_2 axis reveals that there is a significant stabilization of this orbital in the *trans*-fluorine complex, implying a donation of electron density from dinitrogen to the metal along a σ-path enhanced by increasing electronegativity of the *trans*-halogen. The possibility of electron density donation via a σ-path had been discussed by Ruddy and coworkers in 2018;[24a] however, to the best of our knowledge, this is the first time it is identified in a series of transition metal dinitrogen complexes.

The σ-drain of the electron density over both the metal and the dinitrogen bridge is confirmed by a correlation between the decrease in σ orbital energy and the N–N stretching frequency shown in Figure 8. These two parameters correlate with a determination coefficient of ca. 0.99, which further supports that the weakening of the dinitrogen bond is indeed caused by a weakening of the σ interactions due to the electronegativity

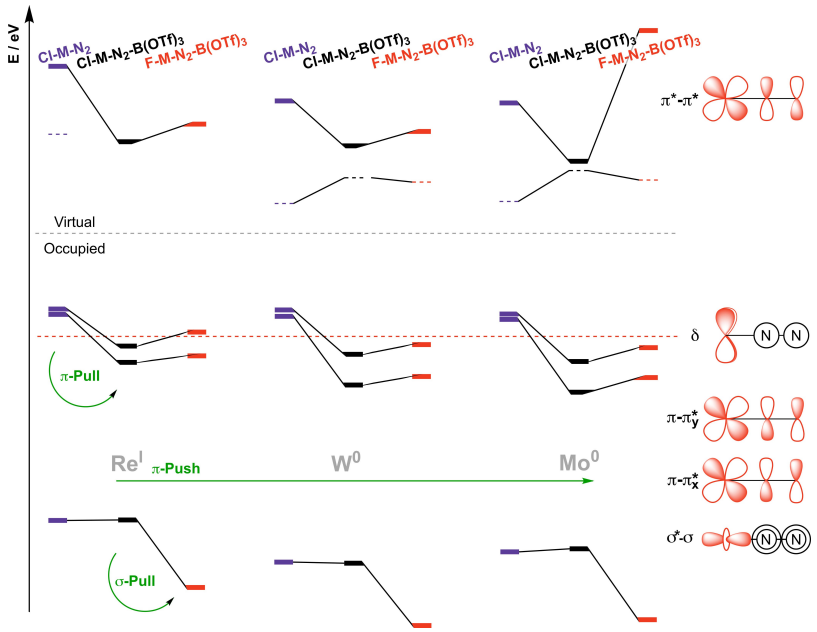

Figure 7. Frontier orbital diagram for the bare Re^{I}, W^0 and Mo^0 complexes (purple) and respective Push/Pull Lewis acid analogues with chloride (black) and fluoride (orange) ligands in the *trans* position relative to the nitrogen.

Research Article
doi.org/10.1002/ejic.202300268

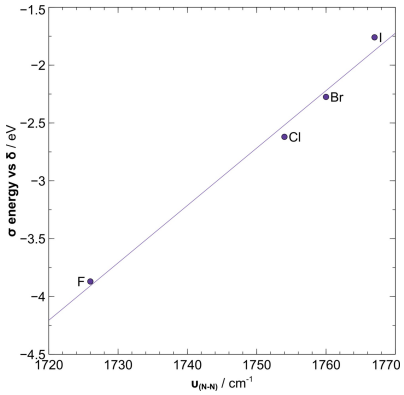

Figure 8. Relative energy of the halogen-metal-N_2 σ orbital with respect to the metal δ orbital, for each X-Re^{I}-N_2-B(OTf)$_3$ adduct, plotted against the respective N–N stretching frequency. Linear fit parameters: $y = 0.0496x - 89.573$, $R^2 = 0.9886$.

of the halogen. The σ effect is stronger than the influence of the metal and compensates for the diminished π-pushing of the metal *d* orbitals. However, the synthetic viability of a fluoride substituent cannot be assessed here; other choices of ligand positioned *trans* to the dinitrogen unit and able to pull electron density via the σ-channel may have a smaller effect.

Conclusions

The activation of the N–N bond and the incorporation of nitrogen atoms into value-added products remains a challenge in chemistry. Computational chemistry can contribute to the design of complexes for dinitrogen activation and transformation by studying the nature of the interactions and ways in which they may be tuned for optimal reactivity.

Herein, we studied the cooperative "push-pull" effect of Lewis acid binding to dinitrogen bound in molybdenum, tungsten and rhenium complexes with a d^6 configuration. Stronger Lewis acids weaken the dinitrogen bond more strongly as monitored by the N–N stretching frequencies, although steric hindrance and electronic effects cannot be fully disentangled. The "push-pull" effect was rationalized with an electronic structure analysis: occupied molecular orbitals with π antibonding interactions between the two nitrogen atoms are more strongly stabilized for stronger Lewis acids. The choice of Lewis acid was furthermore found to determine the orbital ordering in the rhenium complexes. The π*–π* metal-N_2 orbital can be moved into the LUMO position, implying electrochemical bond activation in a single reduction event.

A variation of halides in the *trans*-position to the dinitrogen unit suggested that there are independent σ and π paths that can be used to push or pull electron density from the metal to the dinitrogen ligand. This effect is orthogonal to the Lewis acid effect so that these electronic structure modulations could be harnessed in a cooperative manner to optimally tune a transition metal complex for thermal, electrochemical or even photochemical dinitrogen activation reactivity. To the best of our knowledge, this dichotomy of σ and π "push-pull" paths has not been described before.

With all these results in mind, some guiding principles can be summarized: (1) greater Lewis acid strength is expected to lead to stronger dinitrogen activation via the π path, although the FIA or HIA cannot be used as a simple predictive quantity given that electronics and sterics will interplay, (2) exploring ligand variations in the binding site *trans* to the dinitrogen unit may facilitate orthogonal tuning via the σ path, (3) competing binding sites of LAs need to be evaluated, and strategies to overcome undesired LA binding may be needed, and (4) electrochemical functionalization of the nitrogen atoms may become accessible by LA co-activation.

Experimental Section

Density Functional Theory[41] calculations were performed with the ORCA 5[42] suite of programs. Geometry optimizations and numerical frequency calculations were performed with the functional combining the exchange energy approximation by Becke[43] and correlation by Perdew[44] (BP86) in combination with the balanced polarized triple-ζ basis set from the Ahlrichs family[45] (def2-TZVP) for all atoms. The resolution of the identity integral method,[46] with the appropriate auxiliary basis (def2/J), was used in order to optimize computational cost. Grimme's DFT-D4[47] was included to account for dispersion interactions. Solvent effects were considered using the conductor-like polarizable continuum model (CPCM)[48] for dichloromethane. Explicit solvent molecules are not expected to have a significant influence on the covalent binding reported here and are therefore not included. Equally, counterions and other species commonly found in solution are not explicitly included.

A pincer ligand system by Schneider and coworkers has proven successful in dinitrogen activation using multiple strategies with different transition metal ions.[13b,34b–c,39,49] Redox potentials were calculated using the method described by Schneider and coworkers.[39] The potential is obtained from the difference between the oxidized and reduced forms Gibbs energies and the Nernst equation; a detailed description is given in the SI. It is anchored to the experimental value measured for the first (reversible) wave of *mer*-[ReCl(N_2)(PPhCPh=CPh)(PMe_2Ph)$_3$] (0.19 V vs SCE).[50] The data required to reproduce the plots in this work can be found in the Supporting Information. All the computational data have been uploaded (DOI: 10.19061/iochem-bd-4-56, link: https://doi.org/10.19061/iochem-bd-4-56) onto the ioChem-BD[51] platform (www.iochem-bd.org) to facilitate data exchange and dissemination, according to the FAIR[52] principles of OpenData sharing.

Supporting Information

The authors have cited additional references within the Supporting Information.[39,50,53]

Acknowledgements

The work has been performed under the Project HPC-EUROPA3 (INFRAIA-2016-1-730897), with the support of the EC Research Innovation Action under the H2020 Programme; in particular, FFM gratefully acknowledges the computer resources and

technical support provided by HLRS HPC Center Stuttgart. FFM would also like to thank AEI/MCIN (10.13039/501100011033) for funding (CTQ2017-87392-P, PID2020-114548GB-I00), and a PhD studentship (PRE2018-083883). The Lichtenberg HPC of TU Darmstadt is gratefully acknowledged. Open Access funding enabled and organized by Projekt DEAL.

Conflict of Interests

The authors declare no conflict of interest.

Data Availability Statement

The data that support the findings of this study are openly available in www.iochem-bd.org at 10.19061/iochem-bd-4-56, reference number 4506.

Keywords: Nitrogen Activation · Lewis Acids · Transition Metal Complexes · Push-Pull Effect · Electronic Structure

[1] S. Wendeborn, *Angew. Chem. Int. Ed.* **2020**, *59*, 2182–2202.
[2] J. W. Erisman, M. A. Sutton, J. Galloway, Z. Klimont, W. Winiwarter, *Nat. Geosci.* **2008**, *1*, 636–639.
[3] N. Cherkasov, A. O. Ibhadon, P. Fitzpatrick, *Chem. Eng. Process.* **2015**, *90*, 24–33.
[4] J. G. Chen, R. M. Crooks, L. C. Seefeldt, K. L. Bren, R. M. Bullock, M. Y. Darensbourg, P. L. Holland, B. Hoffman, M. J. Janik, A. K. Jones, M. G. Kanatzidis, P. King, K. M. Lancaster, S. V. Lymar, P. Pfromm, W. F. Schneider, R. R. Schrock, *Science* **2018**, *360*, eaar6611.
[5] IUPAC Top Ten Emerging Technologies in Chemistry 2021, *Vol. 2022*, 2021 ed., International Union of Pure and Applied Chemistry, **2021**.
[6] J. Chatt, J. Chatt, G. E. Fogg, *Proc. R. Soc. London Ser. B* **1969**, *172*, 327–337.
[7] B. M. Hoffman, D. Lukoyanov, Z.-Y. Yang, D. R. Dean, L. C. Seefeldt, *Chem. Rev.* **2014**, *114*, 4041–4062.
[8] a) C. E. Laplaza, C. C. Cummins, *Science* **1995**, *268*, 861–863; b) Y. Sekiguchi, S. Kuriyama, A. Eizawa, K. Arashiba, K. Nakajima, Y. Nishibayashi, *Chem. Commun.* **2017**, *53*, 12040–12043; c) Y. Ohki, K. Munakata, Y. Matsuoka, R. Hara, M. Kachi, K. Uchida, M. Tada, R. E. Cramer, W. M. C. Sameera, T. Takayama, Y. Sakai, S. Kuriyama, Y. Nishibayashi, K. Tanifuji, *Nature* **2022**, *607*, 86–90; d) H. Tanaka, S. Hitaoka, K. Umehara, K. Yoshizawa, S. Kuwata, *Eur. J. Inorg. Chem.* **2020**, *2020*, 1472–1482; e) T. Hatanaka, H. Kusunose, H. Kawaguchi, Y. Funahashi, *Eur. J. Inorg. Chem.* **2020**, *2020*, 1449–1455; f) S. Bennaamane, M. F. Espada, I. Yagoub, N. Saffon-Merceron, N. Nebra, M. Fustier-Boutignon, E. Clot, N. Mézailles, *Eur. J. Inorg. Chem.* **2020**, 1499–1505; g) M. Pfeil, T. A. Engesser, A. Koch, J. Junge, J. Krahmer, C. Näther, F. Tuczek, *Eur. J. Inorg. Chem.* **2020**, *2020*, 1437–1448; h) A. L. Speelman, I. Čorić, C. Van Stappen, S. DeBeer, B. Q. Mercado, P. L. Holland, *J. Am. Chem. Soc.* **2019**, *141*, 13148–13157; i) J. E. Weber, F. Hasanayn, M. Fataftah, B. Q. Mercado, R. H. Crabtree, P. L. Holland, *Inorg. Chem.* **2021**, *60*, 6115–6124; j) Q. J. Bruch, G. P. Connor, N. D. McMillion, A. S. Goldman, F. Hasanayn, P. L. Holland, A. J. M. Miller, *ACS Catal.* **2020**, *10*, 10826–10846.
[9] a) S. Kim, F. Loose, P. J. Chirik, *Chem. Rev.* **2020**, *120*, 5637–5681; b) D. Singh, W. R. Buratto, J. F. Torres, L. J. Murray, *Chem. Rev.* **2020**, *120*, 5517–5581; c) M. J. Chalkley, M. W. Drover, J. C. Peters, *Chem. Rev.* **2020**, *120*, 5582–5636.
[10] J. E. Weber, S. M. Bhutto, A. T. Y. Genoux, P. L. Holland, *Reference Module in Chemistry, Molecular Sciences and Chemical Engineering*, Elsevier, **2021**.
[11] a) S. J. K. Forrest, B. Schluschaß, E. Y. Yuzik-Klimova, S. Schneider, *Chem. Rev.* **2021**, *121*, 6522–6587; b) G. Zhang, T. Liu, J. Song, Y. Quan, L. Jin, M. Si, Q. Liao, *J. Am. Chem. Soc.* **2022**, *144*, 2444–2449; c) F. Meng, S. Kuriyama, H. Tanaka, A. Egi, K. Yoshizawa, Y. Nishibayashi, *Angew. Chem. Int. Ed.* **2021**, *60*, 13906–13912.
[12] V. Krewald, *Dalton Trans.* **2018**, *47*, 10320–10329.
[13] a) F. Schendzielorz, M. Finger, J. Abbenseth, C. Würtele, V. Krewald, S. Schneider, *Angew. Chem. Int. Ed.* **2019**, *58*, 830–834; b) R. S. van Alten, F. Wätjen, S. Demeshko, A. J. M. Miller, C. Würtele, I. Siewert, S. Schneider, *Eur. J. Inorg. Chem.* **2020**, 1402–1410; c) G. C. Stephan, C. Sivasankar, F. Studt, F. Tuczek, *Chem. Eur. J.* **2008**, *14*, 644–652.
[14] a) Y. Tanabe, Y. Nishibayashi, *Coord. Chem. Rev.* **2013**, *257*, 2551–2564; b) H. Broda, S. Hinrichsen, F. Tuczek, *Coord. Chem. Rev.* **2013**, *257*, 587–598; c) R. J. Burford, A. Yeo, M. D. Fryzuk, *Coord. Chem. Rev.* **2017**, *334*, 84–99; d) B. M. Flöser, F. Tuczek, *Coord. Chem. Rev.* **2017**, *345*, 263–280; e) R. J. Burford, M. D. Fryzuk, *Nat. Chem. Rev.* **2017**, *1*, 0026; f) A. Eizawa, Y. Nishibayashi, *Nitrogen Fixation* (Ed.: Y. Nishibayashi), Springer International Publishing, Cham, **2017**, pp. 153–169; g) I. Klopsch, E. Y. Yuzik-Klimova, S. Schneider, *Nitrogen Fixation* (Ed.: Y. Nishibayashi), Springer International Publishing, Cham, **2017**, pp. 71–112; h) H. Tanaka, K. Yoshizawa, *Nitrogen Fixation* (Ed.: Y. Nishibayashi), Springer International Publishing, Cham, **2017**, pp. 171–196.
[15] a) M.-E. Moret, J. C. Peters, *Angew. Chem. Int. Ed.* **2011**, *50*, 2063–2067; b) J. Takaya, *Chem. Sci.* **2021**, *12*, 1964–1981; c) R. C. Cammarota, L. J. Clouston, C. C. Lu, *Coord. Chem. Rev.* **2017**, *334*, 100–111.
[16] a) B. Chatterjee, W.-C. Chang, S. Jena, C. Werlé, *ACS Catal.* **2020**, *10*, 14024–14055; b) B. J. Elvers, S. Pätsch, S. S. M. Bandaru, V. Krewald, C. Schulzke, C. Fischer, *Angew. Chem. Int. Ed.* **2023**, *62*, e202303151; c) L. R. Doyle, A. J. Wooles, S. T. Liddle, *Angew. Chem. Int. Ed.* **2019**, *58*, 6674–6677; d) B. Askevold, J. T. Nieto, S. Tussupbayev, M. Diefenbach, E. Herdtweck, M. C. Holthausen, S. Schneider, *Nat. Chem.* **2011**, *3*, 532–537; e) S. Gambarotta, J. Scott, *Angew. Chem. Int. Ed.* **2004**, *43*, 5298–5308; f) U. J. Kilgore, X. Yang, J. Tomaszewski, J. C. Huffman, D. J. Mindiola, *Inorg. Chem.* **2006**, *45*, 10712–10721.
[17] a) D. Y. Bae, G. Lee, E. Lee, *Inorg. Chem.* **2021**, *60*, 12813–12822; b) Y. Nishibayashi, S. Iwai, M. Hidai, *Science* **1998**, *279*, 540–542.
[18] R. Robson, *Inorg. Chem.* **1974**, *13*, 475–479.
[19] a) M. Mercer, R. H. Crabtree, R. L. Richards, *J. Chem. Soc. Chem. Commun.* **1973**, 808–809; b) M. Mercer, *J. Chem. Soc. Dalton Trans.* **1974**, 1637–1640.
[20] Q.-F. Zhang, J. L. C. Chim, W. Lai, W.-T. Wong, W.-H. Leung, *Inorg. Chem.* **2001**, *40*, 2470–2471.
[21] P. Muller, *Pure Appl. Chem.* **1994**, *66*, 1077–1184.
[22] a) J. P. Shanahan, N. K. Szymczak, *Organometallics* **2020**, *39*, 4297–4306; b) L. Shi, Q. Li, C. Ling, Y. Zhang, Y. Ouyang, X. Bai, J. Wang, *J. Mater. Chem. A* **2019**, *7*, 4865–4871; c) S. N. Khan, A. Kalemos, E. Miliordos, *J. Phys. Chem. C* **2019**, *123*, 21548–21553; d) A. M. Rouf, C. Dai, S. Dong, J. Zhu, *Inorg. Chem.* **2020**, *59*, 11770–11781; e) F. Wech, U. Gellrich, *ACS Catal.* **2022**, 5388–5396.
[23] a) D. Specklin, A. Coffinet, L. Vendier, I. del Rosal, C. Dinoi, A. Simonneau, *Inorg. Chem.* **2021**, *60*, 5545–5562; b) J. P. Shanahan, N. K. Szymczak, *J. Am. Chem. Soc.* **2019**, *141*, 8550–8556; c) J. B. Geri, J. P. Shanahan, N. K. Szymczak, *J. Am. Chem. Soc.* **2017**, *139*, 5952–5956; d) A. S. Coffinet, A. Simonneau, D. Specklin, *Encyclopedia of Inorganic and Bioinorganic Chemistry* (Ed.: R. A. Scott), Wiley, Hoboken, **2020**, pp. 1–25.
[24] a) A. J. Ruddy, D. M. C. Ould, P. D. Newman, R. L. Melen, *Dalton Trans.* **2018**, *47*, 10377–10381; b) A. Simonneau, M. Etienne, *Chem. Eur. J.* **2018**, *24*, 12458–12463.
[25] D. L. J. Broere, P. L. Holland, *Science* **2018**, *359*, 871–871.
[26] a) M.-A. Légaré, G. Bélanger-Chabot, R. D. Dewhurst, E. Welz, I. Krummenacher, B. Engels, H. Braunschweig, *Science* **2018**, *359*, 896–900; b) H. Zhang, R. Yuan, W. Wu, Y. Mo, *Chem. Eur. J.* **2020**, *26*, 2619–2625.
[27] a) J. Zhu, *Chem. Asian J.* **2019**, *14*, 1413–1417; b) A. M. Rouf, C. Dai, F. Xu, J. Zhu, *Adv. Theory Simul.* **2020**, *3*, 1900205; c) C. Dai, Y. Huang, J. Zhu, *Organometallics* **2022**, *41*, 1480–1487; d) A. M. Rouf, Y. Huang, S. Dong, J. Zhu, *Inorg. Chem.* **2021**, *60*, 5598–5606.
[28] a) J. Chatt, J. R. Dilworth, G. J. Leigh, *J. Chem. Soc. D* **1969**, 687–688; b) G. A. Neyhart, K. Seward, B. P. Sullivan, *Inorg. Synth.* **1996**, pp. 262–267.
[29] a) S. Donovan-Mtunzi, R. L. Richards, J. Mason, *J. Chem. Soc. Dalton Trans.* **1984**, 2429–2433; b) J. Chatt, R. C. Fay, R. L. Richards, *J. Chem. Soc. A* **1971**, 702–704.
[30] a) Z.-J. Lv, J. Wei, W.-X. Zhang, P. Chen, D. Deng, Z.-J. Shi, Z. Xi, *Natl. Sci. Rev.* **2020**, *7*, 1564–1583; b) N. Khoenkhoen, B. de Bruin, J. N. H. Reek, W. I. Dzik, *Eur. J. Inorg. Chem.* **2015**, *2015*, 567–598.
[31] J. Junge, S. Froitzheim, T. A. Engesser, J. Krahmer, C. Näther, N. Le Poul, F. Tuczek, *Dalton Trans.* **2022**, *51*, 6166–6176.

[32] a) L. Greb, *Chem. Eur. J.* **2018**, *24*, 17881–17896; bR. J. Mayer, N. Hampel, A. R. Ofial, *Chem. Eur. J.* **2021**, *27*, 4070–4080.
[33] J. Gaffen, *Chem* **2019**, *5*, 1355–1356.
[34] a) S. Rupp, F. Plasser, V. Krewald, *Eur. J. Inorg. Chem.* **2020**, *2020*, 1506–1518; b) L. Alig, K. A. Eisenlohr, Y. Zelenkova, S. Rosendahl, R. Herbst-Irmer, S. Demeshko, M. C. Holthausen, S. Schneider, *Angew. Chem. Int. Ed.* **2022**, *61*, e202113340; c) B. Schluschaß, J.-H. Borter, S. Rupp, S. Demeshko, C. Herwig, C. Limberg, N. A. Maciulis, J. Schneider, C. Würtele, V. Krewald, D. Schwarzer, S. Schneider, *JACS Au* **2021**, *1*, 879–894; d) Y. Wasada-Tsutsui, H. Wasada, T. Suzuki, A. Katayama, Y. Kajita, T. Inomata, T. Ozawa, H. Masuda, *Eur. J. Inorg. Chem.* **2020**, *2020*, 1411–1417; e) M. Fritz, S. Rupp, C. I. Kiene, S. Kisan, J. Telser, C. Würtele, V. Krewald, S. Schneider, *Angew. Chem. Int. Ed. 61*, e202205922; f) A. S. Huss, J. J. Curley, C. C. Cummins, D. A. Blank, *J. Phys. Chem. B* **2013**, *117*, 1429–1436; g) G. Christian, R. Stranger, B. F. Yates, *Chem. Eur. J.* **2009**, *15*, 646–655; h) S. Hinrichsen, A.-C. Schnoor, K. Grund, B. Flöser, A. Schlimm, C. Näther, J. Krahmer, F. Tuczek, *Dalton Trans.* **2016**, *45*, 14801–14813.
[35] A. Egi, H. Tanaka, A. Konomi, Y. Nishibayashi, K. Yoshizawa, *Eur. J. Inorg. Chem.* **2020**, 1490–1498.
[36] a) D. Pun, E. Lobkovsky, P. J. Chirik, *J. Am. Chem. Soc.* **2008**, *130*, 6047–6054; b) I. Vidyaratne, S. Gambarotta, I. Korobkov, P. H. M. Budzelaar, *Inorg. Chem.* **2005**, *44*, 1187–1189; c) I. Vidyaratne, J. Scott, S. Gambarotta, P. H. M. Budzelaar, *Inorg. Chem.* **2007**, *46*, 7040–7049.
[37] P. L. Holland, *Dalton Trans.* **2010**, *39*, 5415–5425.
[38] J. C. Peters, J.-P. F. Cherry, J. C. Thomas, L. Baraldo, D. J. Mindiola, W. M. Davis, C. C. Cummins, *J. Am. Chem. Soc.* **1999**, *121*, 10053–10067.
[39] B. M. Lindley, R. S. van Alten, M. Finger, F. Schendzielorz, C. Würtele, A. J. M. Miller, I. Siewert, S. Schneider, *J. Am. Chem. Soc.* **2018**, *140*, 7922–7935.
[40] N. Stucke, T. Weyrich, M. Pfeil, K. Grund, A. Kindjajev, F. Tuczek, *Nitrogen Fixation* (Ed.: Y. Nishibayashi), Springer International Publishing, Cham, **2017**, pp. 113–152.
[41] R. G. Parr, *Horizons of Quantum Chemistry* (Eds.: K. Fukui, B. Pullman), Springer Netherlands, Dordrecht, **1980**, pp. 5–15.
[42] a) F. Neese, *WIREs Comput. Mol. Sci.* **2012**, *2*, 73–78; b) F. Neese, *WIREs Comput Mol Sci.* **2022**, *12*, e1606; c) F. Neese, F. Wennmohs, U. Becker, C. Riplinger, *J. Chem. Phys.* **2020**, *152*, 224108.
[43] A. D. Becke, *Phys. Rev. A* **1988**, *38*, 3098–3100.
[44] J. P. Perdew, *Phys. Rev. B* **1986**, *33*, 8822–8824.
[45] F. Weigend, R. Ahlrichs, *Phys. Chem. Chem. Phys.* **2005**, *7*, 3297–3305.
[46] R. A. Kendall, H. A. Früchtl, *Theor. Chem. Acc.* **1997**, *97*, 158–163.
[47] E. Caldeweyher, C. Bannwarth, S. Grimme, *J. Chem. Phys.* **2017**, *147*, 034112.
[48] V. Barone, M. Cossi, *J. Chem. Phys. A* **1998**, *102*, 1995–2001.
[49] Q. J. Bruch, B. M. Lindley, B. Askevold, S. Schneider, A. J. M. Miller, *Inorg. Chem.* **2018**, *57*, 1964–1975.
[50] A. J. L. Pombeiro, M. Teresa, A. R. S. Costa, Y. Wang, J. F. Nixon, *J. Chem. Soc. Dalton Trans.* **1999**, 3755–3758.
[51] M. Álvarez-Moreno, C. de Graaf, N. López, F. Maseras, J. M. Poblet, C. Bo, *J. Chem. Inf. Model.* **2015**, *55*, 95–103.
[52] M. D. Wilkinson, M. Dumontier, I. J. Aalbersberg, G. Appleton, M. Axton, A. Baak, N. Blomberg, J.-W. Boiten, L. B. da Silva Santos, P. E. Bourne, J. Bouwman, A. J. Brookes, T. Clark, M. Crosas, I. Dillo, O. Dumon, S. Edmunds, C. T. Evelo, R. Finkers, A. Gonzalez-Beltran, A. J. G. Gray, P. Groth, C. Goble, J. S. Grethe, J. Heringa, P. A. C.'t Hoen, R. Hooft, T. Kuhn, R. Kok, J. Kok, S. J. Lusher, M. E. Martone, A. Mons, A. L. Packer, B. Persson, P. Rocca-Serra, M. Roos, R. van Schaik, S.-A. Sansone, E. Schultes, T. Sengstag, T. Slater, G. Strawn, M. A. Swertz, M. Thompson, J. van der Lei, E. van Mulligen, J. Velterop, A. Waagmeester, P. Wittenburg, K. Wolstencroft, J. Zhao, B. Mons, *Sci. Data* **2016**, *3*, 160018.
[53] a) P. Erdmann, J. Leitner, J. Schwarz, L. Greb, *ChemPhysChem* **2020**, *21*, 987–994; b) E. R. Clark, A. Del Grosso, M. J. Ingleson, *Chem. Eur. J.* **2013**, *19*, 2462–2466.

Manuscript received: May 8, 2023
Revised manuscript received: September 5, 2023
Accepted manuscript online: September 15, 2023
Version of record online: October 12, 2023